



## Testing micro-channel plate detectors for the particle identification upgrade of LHCb

L. Castillo García<sup>a,b,\*</sup>

<sup>a</sup> CERN, CH 1211 Geneva 23, Switzerland

<sup>b</sup> Universidad de Granada, ES 18071 Granada, España

On behalf of the LHCb-RICH Collaboration<sup>1</sup>

### ARTICLE INFO

Available online 31 December 2011

#### Keywords:

LHCb upgrade  
TORCH detector  
Cherenkov light  
Micro-channel plate photomultiplier tubes  
Single photons

### ABSTRACT

The TORCH, Time of internally Reflected Cherenkov Light, is proposed for the high luminosity upgrade of the LHCb experiment. The detector combines Time-of-Flight and Cherenkov techniques to achieve positive  $\pi/K/p$  separation on a  $\geq 3\sigma$  level in the momentum range below 10 GeV/c. The required time resolution is  $\leq 50$  ps for single photon signal.

In a preliminary R&D phase, we have shown that already commercially available micro-channel plate tubes with  $8 \times 8$  channels fulfil the requirements. Timing properties of the tubes have been investigated with a pulsed laser diode in single photon regime. Key results from these laboratory tests are reported. An excellent timing resolution of  $< 40$  ps is achieved with an efficiency of  $\sim 90\%$ .

© 2011 Elsevier B.V. All rights reserved.

## 1. Introduction

The TORCH detector [1] is proposed for particle identification at low momentum within the LHCb upgrade framework [2]. It will use time-of-flight information from Cherenkov light generated by charged particles crossing a 1 cm-thick quartz plane. The photons propagate by total internal reflection to the edge of the plane and are focused onto an array of micro-channel plate (MCP) photon detectors, where their arrival would be timed (Fig. 1). Micro-channel plate photon detectors are currently the best choice for fast timing of single photons. The system requires the development of photon detectors with finely segmented anode and a time spread better than 50 ps for single photons. From simulation studies, it is found that a 128-channel segmentation in one dimension ( $\sim 0.4$  mm) and an angular dynamic range of 400 mrad correspond to an uncertainty per-photon on the time of propagation of  $O(70$  ps) whereas in the other dimension the required granularity is much looser ( $\sim 6.5$  mm).

## 2. Experimental setup

In the current R&D phase commercially-available micro-channel plate photon detectors with segmented anode<sup>1</sup> are being characterized. The anode consists of an array of  $8 \times 8$  pads (5.9/

6.5 mm size/pitch) for a total of  $53 \times 53$  mm<sup>2</sup> active area. The detectors are equipped with two MCP's in chevron configuration with 25  $\mu$ m pore diameter and an overall gain of up to  $10^6$ .

The experimental setup has been partially inspired by the one described in reference [3]. Timing properties of the tubes are investigated with a pulsed laser diode<sup>2</sup> emitting at 405 nm (Fig. 2). The pulse width is 20 ps FWHM and the light is attenuated through neutral density filters to a level of a few single photons. The light is focused by a microfocus lens<sup>3</sup> and a collimator<sup>4</sup>. The best spot size achieved was 200  $\mu$ m FWHM. Single-channel read out electronics was used to read out the output signal from one pad with all other pads connected to ground. Time jitter distribution measurements are performed with a 1 GHz-fast timing amplifier with Constant Fraction Discriminator<sup>5</sup> (CFD). Pulse height spectrum measurements are obtained using a charge preamplifier<sup>6</sup> connected to a spectroscopy shaping amplifier<sup>7</sup> (shaping time 0.5  $\mu$ s). Data were registered in a multi-channel analyzer<sup>8</sup>.

<sup>2</sup> Optical head model PiL040, digital control unit EIG1000D from PiLas, D-12489, Berlin, Germany.

<sup>3</sup> Model PiL040MFS-30 from PiLas.

<sup>4</sup> Model PiL040-FC-6.16 from PiLas.

<sup>5</sup> Model 9327 from ORTEC, Oak Ridge, TN37831-0895, USA.

<sup>6</sup> Model 142 A from ORTEC.

<sup>7</sup> Model 672 from ORTEC.

<sup>8</sup> Model ADCAM 926 MCB (8192 channels) from ORTEC.

\* Corresponding author at: CERN, CH 1211 Geneva 23, Switzerland.

E-mail address: [icastillogarcia@hotmail.com](mailto:icastillogarcia@hotmail.com)

<sup>1</sup> Model XP85012-A1 from Burle/Photonis, Lancaster, PA17601-5688, USA.

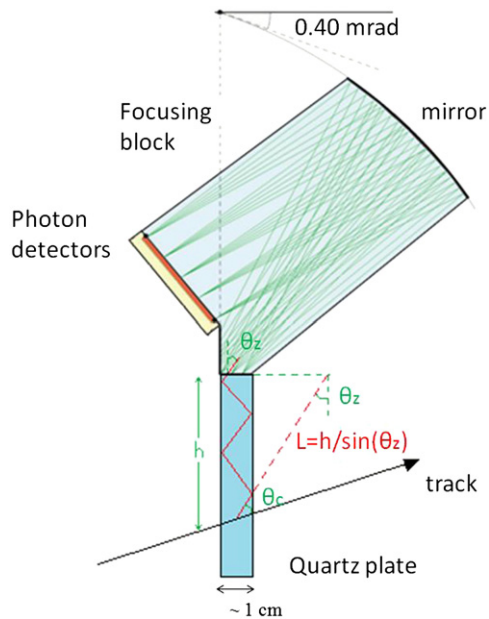


**Fig. 1.** Schematic principle of the TORCH detector. Cross-section through focusing element, attached to the edge of the quartz plate. The focusing of photons is indicated for five illustrative angles between 450 and 850 mrad, emerging at different points across the edge of the plate.

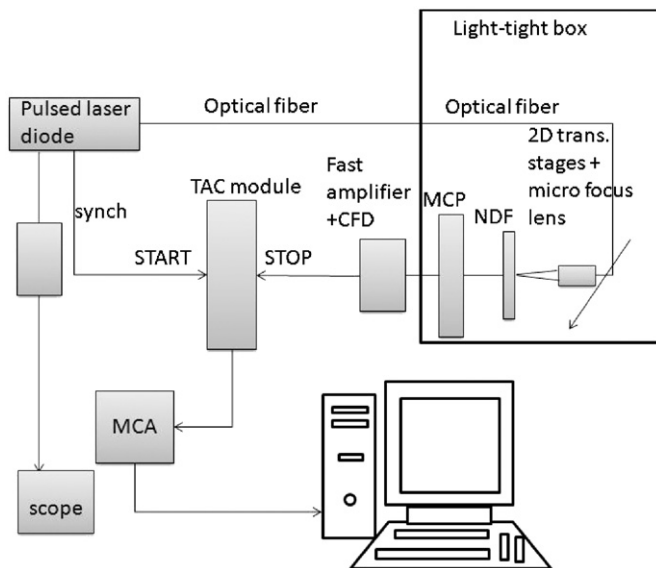


**Fig. 2.** Laboratory set-up used for the systematic studies of the timing performance of the MCP-PMT's.

### 3. Results

#### 3.1. Pulse height spectra and time jitter distributions for single-photoelectrons

The laser intensity is calibrated in photoelectron units by operating the MCP at a rather moderate (non saturated) gain of  $\sim 7 \times 10^5$ . The resulting pulse height spectrum is fitted using a standard Poisson distribution model to infer  $\mu$ , the average number of photoelectrons per pulse. The data points and the fit are in very good agreement over up to five photoelectrons (Fig. 3). The model assumes that the N-photoelectron peak width  $\sigma_{Nphe}$  scales as  $\sigma_{Nphe} = \sqrt{N}\sigma_{1phe}$  where  $\sigma_{1phe}$  is the width of the 1-photoelectron peak. The average number of photoelectrons  $\mu$  is derived

from the probability to have zero photoelectrons and is equal to  $0.51 \pm 0.05$  where uncertainties are estimated by using error propagation.

At the same operating conditions timing measurements are performed. The start time is provided by the laser synchronization signal, and the stop time by the output signal from the CFD. A typical timing distribution is reproduced in Fig. 4. It consists of three parts (from left to right): a main prompt peak, a shoulder on the right of the main peak, and a long tail. The main peak represents the measured intrinsic time response, the shoulder is due to the laser operating mode, and the long tail results from photoelectron back-scattering effects at the MCP input surface. The relative shoulder amplitude was seen to increase with the laser diode intensity while keeping the filters attenuation constant. The laser data sheets indicate that for large intensities, the fast primary light pulse is followed by a wider low-amplitude pulse. The larger the intensity is, the larger the amplitude of this secondary pulse is. A specific measurement provided by the laser manufacturer confirms the existence of this second relaxation oscillation with a time delay of about  $150 \pm 50$  ps. This shoulder was not attributed to back-scattering effects since in this case its relative amplitude should stay constant (or decrease) as the laser light intensity is increased. Given the presence of the shoulder, the timing distribution is fitted with two Gaussians. The time jitter value is inferred from the standard deviation of the first Gaussian at the main peak leading edge and is equal to 38 ps. The tail due to backscattered photoelectrons extends to  $\sim 1.5$  ns from the main signal. This measured value corresponds to a photoelectron being elastically backscattered at an angle of 90 from the MCP input surface. It matches the value estimated from the photocathode-MCP input gap of 4.5 mm and the voltage difference of 350 V. The backscattered photoelectron effect is not dominant as is shown in Fig. 4.

Timing measurements were performed with three different voltage thresholds at the CFD input. The corresponding photoelectron detection efficiencies are estimated by converting the three thresholds in charge units ( $22.5$ ,  $40.5$ , and  $54.0$ )  $\pm 3.3$  fC and by considering the one photoelectron peak in the pulse height spectrum fit (Fig. 5). The corresponding efficiency values are 88%, 93% and 97%.

#### 3.2. Spatial aspects.

##### 3.2.1. Point spread function

The point spread function is studied using X-Y translation stages to scan the laser light pencil along the axial lines of the pad. For each laser position, a pulse height measurement is performed, and the corresponding average charge signal amplitude is determined (Fig. 6). Spatial scans result in a point spread function value of  $\sim 1$  mm FWHM at the anode level. This value already matches the fine granularity of 0.4 mm required by the TORCH design. It can be reduced by decreasing the gap distance (currently  $3.50 \pm 0.36$  mm) between the MCP output plane and the anode. The periodic oscillation on the central part of the pad is attributed to a spatial beating effect between the two MCP's, as its pitch is comparable to the MCP pre-form dimension.

##### 3.2.2. Scans at the pad boundaries.

The TORCH photon detectors require very finely segmented anodes ( $8 \times 128$  read out pads). It is therefore important to check if the timing performance reported in the previous section is maintained at the pad boundaries. For this purpose, timing distributions were recorded at three specific laser positions: the pad center, edge and corner. The experimental conditions and settings were left unchanged to perform various pulse height

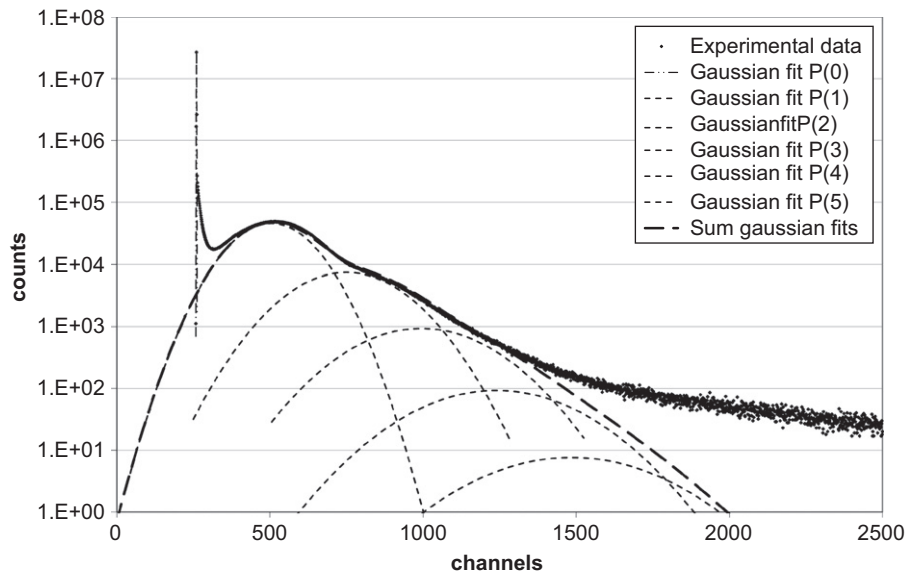


Fig. 3. MCP charge spectrum fitted with a Poisson distribution model.

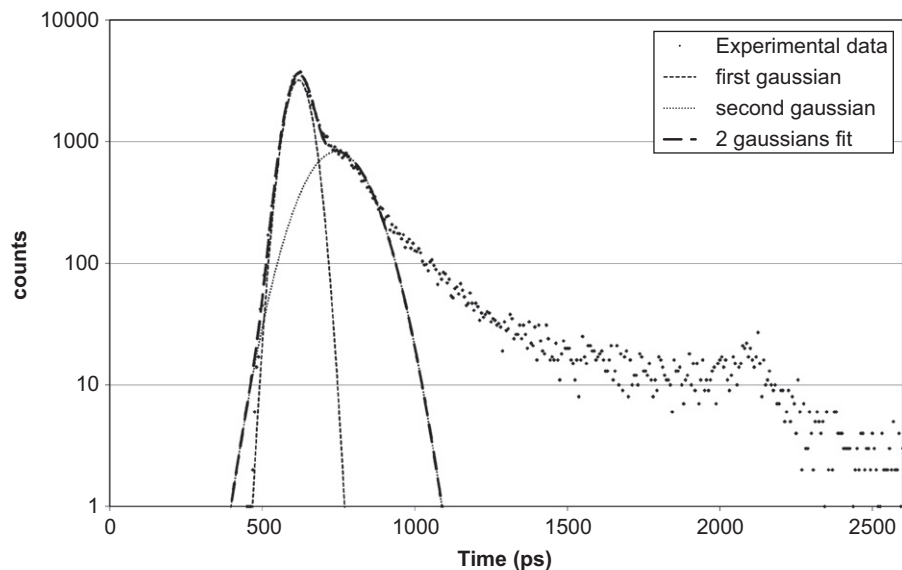


Fig. 4. Single photoelectron timing distribution (vertical logarithmic scale). Prompt signal with a time resolution of  $\sim 38$  ps, shoulder due to the second laser pulse and tail due to backscattered photoelectrons.

spectra and timing measurements at these three positions. As expected, a charge sharing effect is observed. Moving from the center to the edge of the pad, no timing performance degradation is seen within uncertainties. However, since the charge available to the read out pad is reduced, the photoelectron detection efficiency drops accordingly. Table 1 summarizes all these results.

#### 4. Discussion

Many effects contribute to the overall measured time jitter and these add to each other in quadrature. They are:

- jitter between synchronization signal and optical output pulse ( $< 3$  ps)<sup>9</sup>,

- laser pulse width ( $\sim 20$  ps FWHM for the optimal laser tune setting)<sup>9</sup>,
- photoelectron transit time spread between the photocathode and the MCP input (the blue light photoelectron emission velocity spectrum ranges over  $\sim 1$  eV. This corresponds to a time difference of up to  $\sim 50$  ps for a 4.5 mm gap and a voltage of 350 V),
- MCP intrinsic transit time spread,
- amplifier and CFD time slewing (residual walk) as a function of the pulse amplitude (shifts of up to  $\pm 40$  ps, depending on the amplitude range used)<sup>10</sup>,
- CFD timing jitter (20 ps)<sup>10</sup>,
- Multi-channel analyzer channel resolution (6.25 ps).

In the single photoelectron regime, corresponding to low MCP signal amplitudes, the CFD residual time walk contribution is very non-uniform<sup>10</sup>. These residual walk effects have been

<sup>9</sup> Laser diode data sheets from PiLas.

<sup>10</sup> Fig. 1.3 in Model 9327 ORTEC Operating and Service Manual.

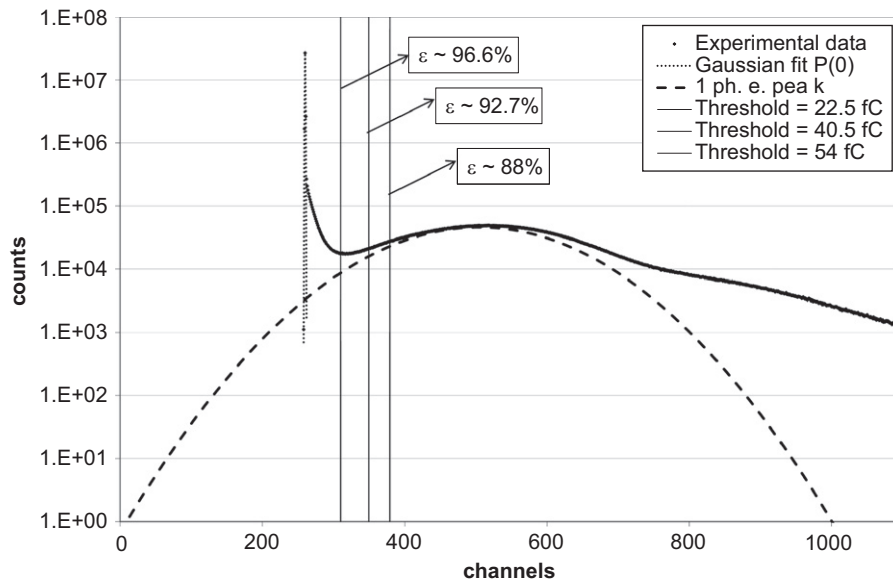


Fig. 5. MCP charge spectrum and efficiency estimate for three thresholds applied at the CFD level.

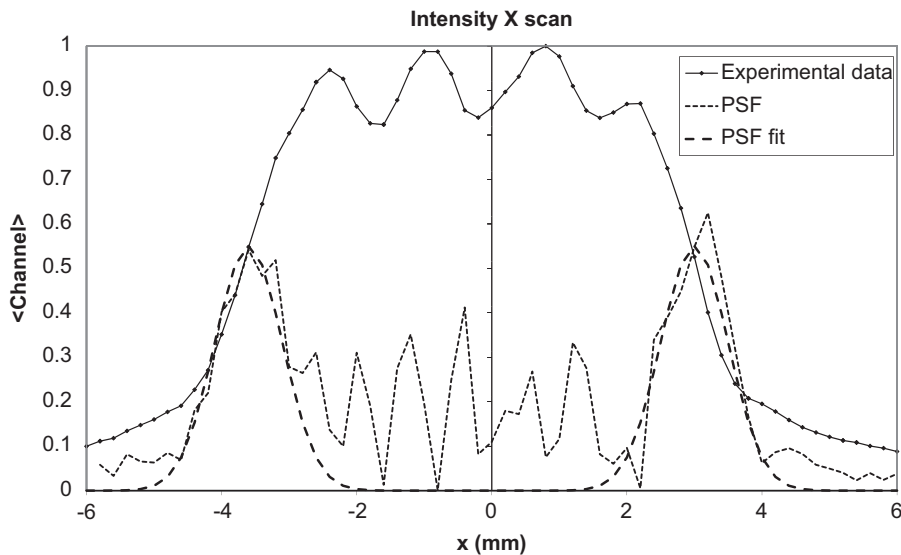


Fig. 6. Average signal amplitude corresponding to a laser scan along a pad axial line. Point spread function inferred from the derivative of the experimental data fitted with a Gaussian model.

Table 1

MCP performance from the laser scans. For three laser positions the estimates of the single photoelectron charge, timing resolution and photoelectron detection efficiency are summarized.

| Laser position | $Q_{1,ph,a}(fc)$ | $\sigma_t(ps)$ | Efficiency range(%) |
|----------------|------------------|----------------|---------------------|
| Center         | ~147.3           | 49             | 90–96               |
| Edge           | ~77.7            | 41             | 75–92               |
| Corner         | ~39.5            | 45             | 29–74               |

investigated in detail by recording timing distributions for various average number of photoelectrons and for three CFD walk settings. In Fig. 7 the main peak position in the timing distribution is plotted against the input signal amplitude converted in mV. The curve is in agreement with the manufacturer's data. It clearly shows that in the single photoelectron regime, residual time

walks combined with MCP signal fluctuations are not negligible and contribute to the overall measured time jitter.

## 5. Conclusions and perspectives

The work reported in this paper shows that the basic TORCH requirements for the photon detectors are fulfilled by commercially-available MCP tubes. For single photoelectrons an excellent timing resolution  $O(<40\text{ ps})$  is obtained with an estimated detection efficiency of  $\sim 90\%$  at the pad center. Timing performance is similar at the pad boundaries with the expected efficiency drop. These results are achieved by operating the MCP at a rather moderate gain of  $7 \times 10^5$ . The laser pulse contribution to timing distributions has been understood and taken into account. Detailed studies of residual time walk effects have been performed and their contribution to the overall time jitter should

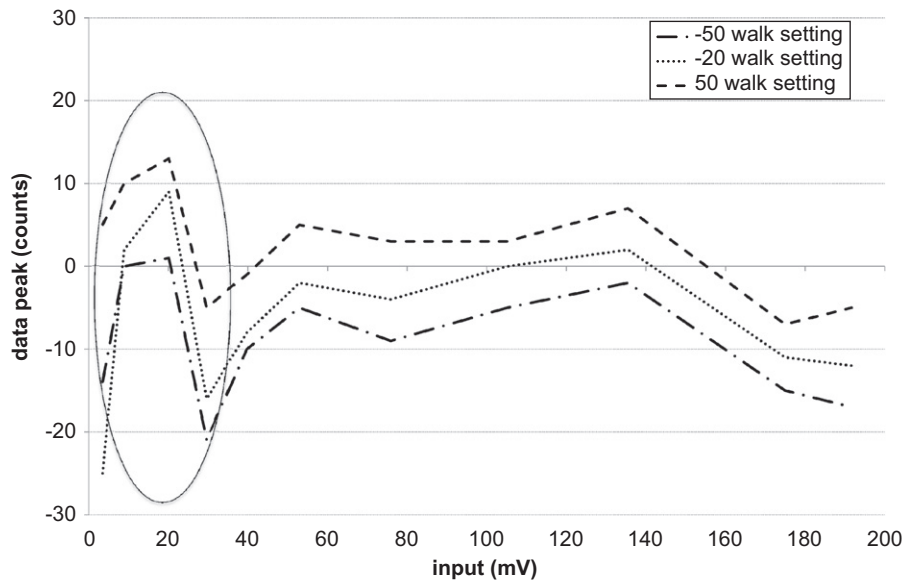


Fig. 7. Time peak position vs MCP input signal amplitude for three different CFD walk settings. The single photoelectron region is denoted by the oval.

be further investigated. The next step is to investigate charge sharing and crosstalk effects in adjacent pads with two-channel electronics read-out. This will allow to define the key design parameters for the final photon detector.

#### Acknowledgments

We are indebted to T. Gys for his aid and support throughout this work. The mechanics and optics was skillfully provided by

D. Piedigrossi. Support from the LHCb collaboration is gratefully acknowledged.

#### References

- [1] M.J. Charles, R. Forty, Nucl. Instr. Meth. A 639 (2011) 173.
- [2] LHCb Collaboration, Letter of Intent publication, CERN-LHCC-2011-001.
- [3] J. Va'vra, et al., Nucl. Instr. Meth. A 595 (2008) 270.